Seismic behaviour of pile groups in sloping ground

S.S.W. Weerasuriya Achchillage
University of Cambridge, Cambridge, UK , ssww2@cam.ac.uk

S.P.G. Madabhushi
University of Cambridge, Cambridge, UK , mspg1@cam.ac.uk

ABSTRACT: With growing interest in offshore energy infrastructure, the seismic stability of structures founded on relatively shallow submarine clay slopes has gained significant attention. These slopes, typically less than 10°, are common in coastal areas supporting wharf structures and quay walls as well as on riverbanks where bridge abutments are founded. While stable under static conditions, they have been associated with large-scale failures under seismic loading. Despite extensive research on pile behaviour in liquefiable sands that suffer lateral spreading, limited attention has been given to pile foundations in soft clay deposits and layered soils. This study investigates the dynamic response of 2×2 pile groups embedded in gently sloping soft clay overlying dense sand. Dynamic centrifuge tests were conducted at Schofield Centre, University of Cambridge on slopes of 3° and 6° under varying seismic intensities and frequencies. Two test configurations, one with negligible pile cap mass and another with substantial mass enabled isolation of kinematic and inertial effects. The results focus on bending moment distributions along pile depth, with particular emphasis on the influence of slope angle.

1 INTRODUCTION

Pile foundations are essential for supporting offshore and onshore structures by transferring loads to deeper, more competent strata while resisting various lateral forces throughout their service life. Their lateral response has been widely studied due to the influence of wind, wave, and seismic loading, as well as slope or embankment instability (Garala and Madabhushi, 2021a, Garala and Madabhushi, 2021b, Haskell et al., 2013).

Under earthquake excitation, pile foundations are subjected to kinematic demands due to deformation and downslope movement of the soil while also being subjected to extra inertial forces and overturning moments due to the oscillation of the superstructure mass. The combined effects of concurrent kinematic and inertial loading on pile foundations are complex and are not yet fully understood, with limited research addressing this interaction comprehensively.

Lateral spreading of gently sloping ground due to liquefaction of loose, saturated sands in seismically active regions has been extensively studied in the past due to the catastrophic damage caused to pile foundations by earthquakes such as the 2016 Kaikoura earthquake in New Zealand and the 2019 Indonesian earthquake (High,2002; Haskell et al., 2013).

However with the growing offshore energy industry, the seismic stability of structures on low-gradient submarine slopes has also recently gained more attention. These slopes often can be present in both shallow coastal waters and deep ocean typically consisting of soft cohesive soils. While they appear stable under static conditions they have been shown to fail catastrophically under seismic loading (Nadim et al.,2007) highlighting the need for improved understanding of pile–soil interaction in such environments. While these slopes, typically less than 10°, are common in near shore areas supporting wharf structures and quay walls they are also present on riverbanks where bridge abutments are founded.

In this study, results from two saturated, dynamic centrifuge tests conducted on 3° and 6° slopes are compared to investigate the influence of slope inclination on the seismic response of pile groups. The experimental methodology developed by Soriano Camelo et al. (2022) to simulate the seismic behaviour of gentle clay slopes was adopted. Each experiment included two 2×2 pile groups: one subjected to kinematic loading only (negligible pile cap mass) and the other to combined kinematic and inertial effects (substantial pile cap mass).

Although the wider research programme investigated pile groups with centre-to-centre spacings of 2.5d and 5d where d is the pile diameter, the present paper focuses on the 5d configuration, with the primary objective of evaluating and quantifying the influence of slope inclination on the dynamic response of the pile groups.

2 CENTRIFUGE MODELLING

2.1 Model design

This study presents the findings of dynamic experiments carried out in the 10 m-diameter Turner beam centrifuge at the Schofield Centre (Madabhushi, 2014), operating at an acceleration of 60*g*. Through centrifuge modelling, small-scale models can accurately reproduce the soil's stress–strain response by increasing the gravitational field by a factor of N (with N = 60 in this case). The correspondence between model-scale and full-scale (prototype) behaviour is defined using scaling laws established by Schofield (1980).

As the problem at hand involved a semi-infinite slope that may involve large deformations under earthquake motions, the laminar container embodying zero lateral stiffness was utilised to prepare the soil models (Brennan et al. 2006). The laminar box is assembled by stacking individual rectangular laminations with cylindrical bearings in between thereby facilitating free displacement of the soil layers in the direction of base shaking.

Box dimensions are 500 mm × 250 mm × 241 mm where box height is dependant of the number of laminations used. The servo-hydraulic shaker was used to simulate the series of earthquakes presented in Table 2 (Madabhushi *et al.*, 2012).

2.2 Materials and model preparation

A layered soil profile where a speswhite kaolin clay layer is underlain by a dense sand layer (relative density = 85 %) using Hostun HN31 sand of d_{50} = 0.325 mm, was prepared. Figure 1 presents the cross-sectional test schematic, with the direction of shaking being right and left.

The 136 mm thick dense sand layer was prepared using an automatic sand pourer (Madabhushi et al., 2006) and was saturated with water from the bottom up using gravity.

The clay slurry was prepared by mixing kaolin clay powder with water at 120 percent of its liquid limit (i.e. approximately double its liquid limit) and was mixed under vacuum to ensure a homogeneous slurry. Table 2 presents material properties of the speswhite kaolin clay. Due to practicality concerns of using the laminar container for the consolidation process, it was carried out in a separate strong box having similar length and width dimensions as the laminar box but with greater depth.

The top of the model was subjected to computer-controlled loading increments whilst suction was applied at the bottom of the model to obtain a depth varying undrained shear strength (s_u) profile. After completion of consolidation, the clay block was trimmed to the required 105mm height and had an unit weight of 16.7 kN/m^3. This was then placed on the saturated dense sand layer in the laminar container .

Table 1. Properties of speswhite kaolin clay (Lau, 2015)

Material property	Value
Liquid limit (%)	30
Plastic limit (%)	63
Specific Gravity, G_s	2.6
Slope of critical state line (CSL) in *q-p`* plane	0.9
Slope of unload reload line (κ)	0.039
Intercept of CSL at $p`$=1 (τ)	3.31
Slope of normal consolidation line (λ)	0.22

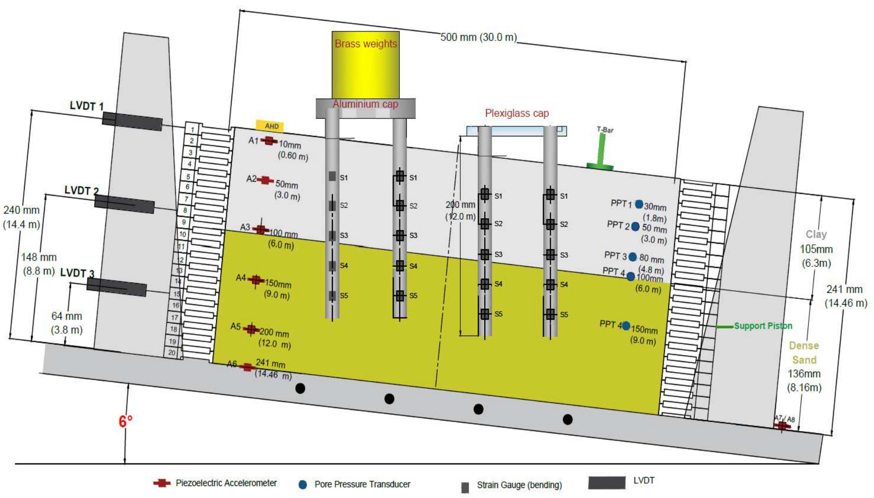

Figure 1. Schematic of centrifuge model at 6°.(prototype dimensions within brackets)

2.3 Model pile foundations

The experiments employed strain-gauged aluminium tubular model piles, measuring 200 mm in length (*l*), with an outer diameter (*d*) of 15 mm and a wall thickness (*t*) of 1 mm, to represent the prototype pile. The prototype's flexural stiffness corresponds to that of a 0.9 m diameter high-strength concrete pile.

Each experiment contained two pile groups, one fitted with a Perspex pile cap and the other with a heavier aluminium cap with added brass weights. As the weight of the Perspex pile cap is negligable compared to that of the piles‘ axial bearing capacity and self-weight it was deemed suitable to assume that the pile groups response was more akin to a purely kinematic interaction (KI only case). The pile group fitted with the brass weights on the other hand weighed 4kg, generating a static vertical load of 2.354 kN at model scale which is equivalent to 8.5 MN at prototype scale. This simulated combined kinematic and inertial interaction (KI+II case).

To simulate the gentle slope the model was tilted using 3° and 6° wedges placed along the base of the model box. The pile groups were then manually installed in the soil model at 1*g* where the pile was embedded in the sand for a depth of 75 mm (~*5d*) to maintain pile fixity conditions. The vertical alignment of the pile heads were maintained throughout the installation process and care was taken to place the two pile groups in separate vertical planes and sufficiently far away from each other to limit dynamic interactions between them.

2.4 Experimental programme and loading sequence

Centrifuge acceleration was progressively increased in increments of 10*g* until the target acceleration of 60*g* was reached. Upon reaching this level, the model was allowed to reconsolidate for approximately 30 minutes prior to seismic loading (equivalent to 75 days in prototype time). Following reconsolidation, a T-bar in-flight characterisation test was conducted to determine the undrained shear strength profile of the clay layer. An air hammer device and accelerometer array was also used to measure shear wave velocities at various depths within the model as per section 3.1.

Figure 2 shows the model loaded onto the centrifuge prior to the test flight. The centrifuge pivot is just out of sight at the top centre of the image, the servo-hydraulic shaker high pressure cylinders are in blue, with most of the shaker body cropped out at the bottom.

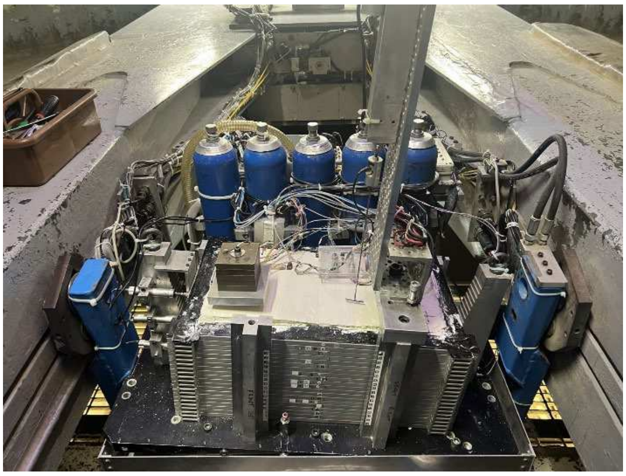

Figure 2. Model box placed in the centrifuge prior to experiment.

Table 2 summarises the earthquake sequences employed in the two experiments. A mixture of real earthquakes and sinusoidal wave motions of a prototype frequency of 1 Hz were fired. A small intensity sine-sweep motion was first carried out to determine the natural frequency of the soil-pile systems. For the purpose of this study only results obtained during EQ6 are considered.

Table 2. Earthquake sequence for experiments.

ID	Earthquake motion	PGA
EQ1	Sine-sweep	0.03g
EQ2	Imperial valley	0.05g
EQ3	Kobe motion	0.3g
EQ4	Sine wave,1 HZ,10 cycles	0.1g
EQ5	Sine wave, 1 Hz ,10 cycles	0.2g
EQ6	Sine wave, 1 Hz ,15 cycles	0.3g

2.5 Instrumentation

Sensors were installed at selecetd depths in the clay and sand layers (Figure 1). Piezoelectric accelerometers and pore pressure transducers were used to measure soil accelerations and pore pressure readings during each earthquake. The upslope and downslope piles were strain gauged to measure bending moment and were waterproofed using two-part epoxy resin. Linearly varying differential transducers (LVDT‘s) were installed on the sides of the model box to measure lateral displacement of the laminations, with further manual reading taken at the end of the flight.

DASYLab v13.0 software was employed to record data into text files for subsequent analysis. During dynamic events, data were logged at a frequency of 6000 Hz, while a rate of 100 Hz was utilised during swing-up to capture pore pressure and settlement variations as the g-level increased from one to sixty.

3 TEST RESULTS

3.1 Strength and stiffness of the soil layer

To determine the undrained shear strength (s_u) of the clay layer, a T-bar test was carried out prior to and after firing the earthquakes at 60*g* (Figure 3(a)). Shear wave velocities measured using the air-hammer device was utilised to calculate the small-strain stiffness (G_0) profile alongside comparable empirical G_0 values computed from Hardin Drenvich (1972), Viggiani and Atkinson (1995) and Oztoprak and Bolton (2013), which are presented in Figure 3(b).

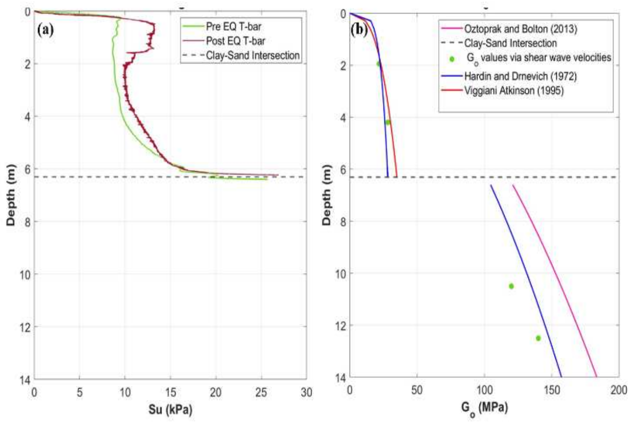

Figure 3. (a) undrained shear strength profile for clay layer (b) maximum shear modulus for soil layers.

The visible initial increase of s_u after the last earthquake may be suggestive of further drying of the clay or may be due to potential reconsolidation over the duration of the application of all five base excitations. Figure 3(b) shows that the experimental and theoretical G_0 profiles are in good agreement with each other.

3.2 Soil lateral displacements

Soil lateral displacements for the 3° and 6° slopes are shown in Figure 4. As expected, the 6° slope produced markedly larger movements compared to its 3° counterpart . The maximum displacement at 6° was approximately three and a half times greater than that at 3°. Horizontal displacements within the clay layer (0.36 m and 5.40 m prototype depths) were substantially higher than those in the underlying dense sand at a depth of 10.38 m. The larger clay displacements are attributed to its lower soil stiffness and higher deformability. In contrast, the dense sand exhibited minimal movement owing to its higher stiffness and confining stress.

3.3 Pile bending moments

Figure 5 illustrates the maximum bending moment envelopes for both upslope and downslope piles within each pile group. The bending moments correspond to various depths along the piles and do not necessarily occur simultaneously. Figures 5(a) and 5(b) present the results for the KI and KI+II cases, respectively, for the model with a 6° slope, while Figures 5(c) and 5(d) show the corresponding results for the 3° slope model.

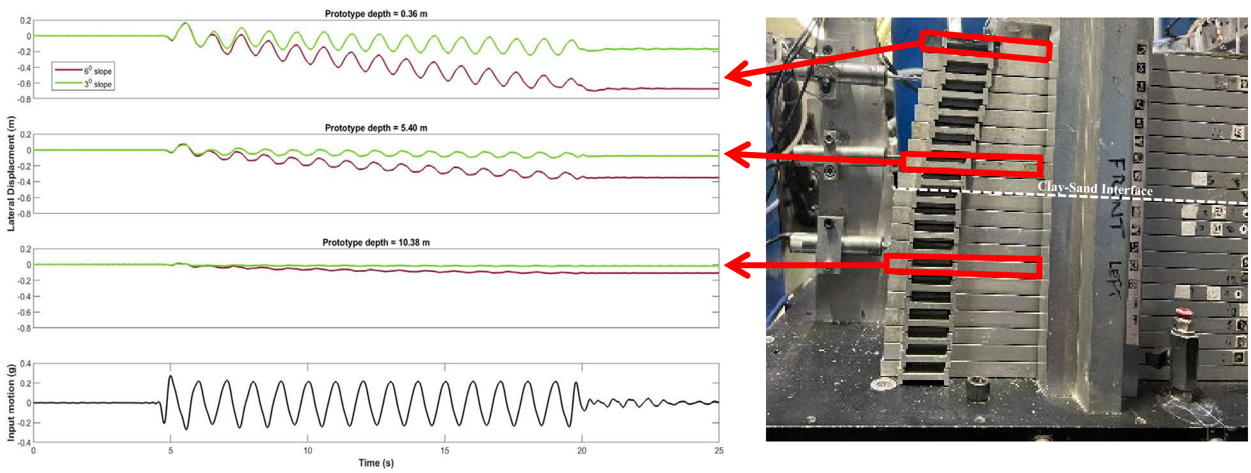

Figure 4. Lateral soil displacements at different depths of the model during EQ6– and time history of EQ6 input motion.

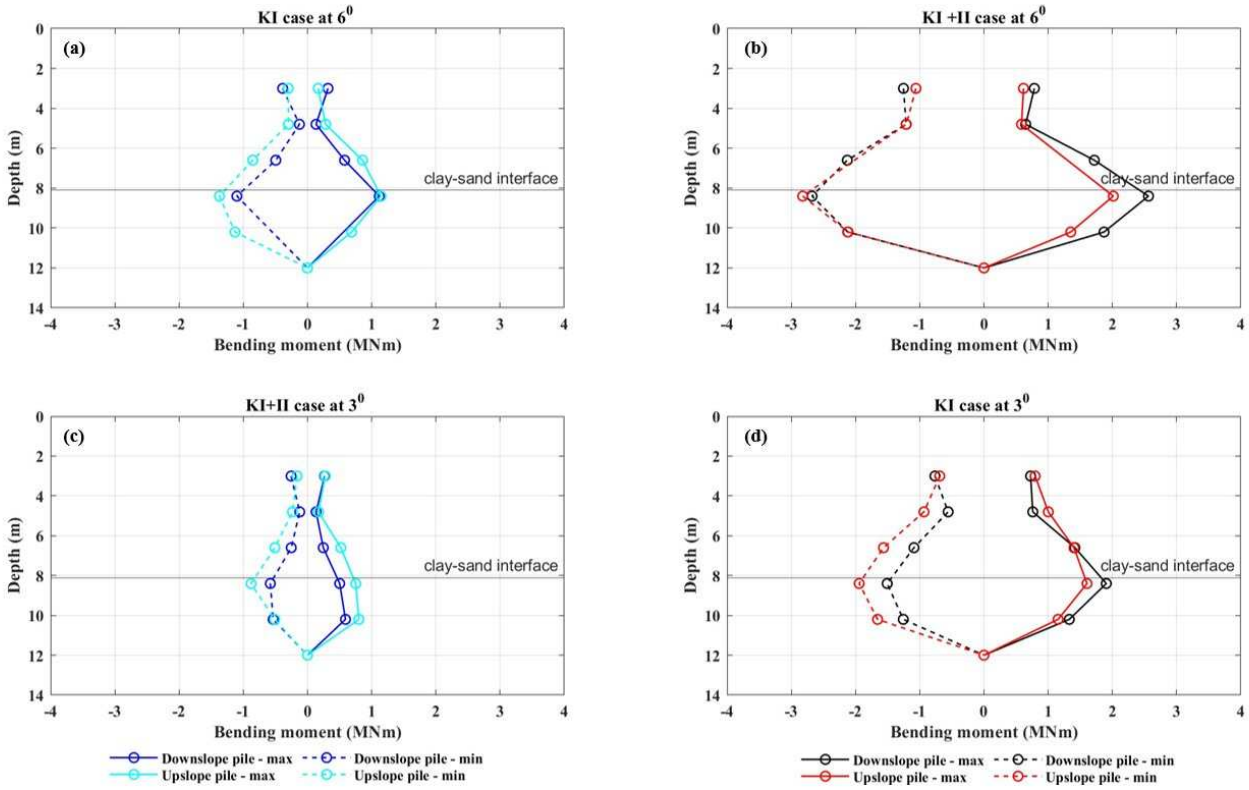

Figure .5 – Bending moment envelopes for uplsope and downslope piles for 3^0 and 6^0.

In all configurations, the upslope piles exhibit the highest bending moments, which is consistent with their direct interaction with the mobilised soil mass during lateral ground movement. The downslope piles in all four scenarios show approximately 22-34% less bending moment than its upslope counterpart due to pile groups shadowing effects.

As expected, introducing the head mass leads to a substantial amplification of bending moments compared with the purely kinematic case, with peak values increasing by approximately 2.0 and 2.3 times for the 6° and 3° slope models, respectively.

Comparing the KI + II results between the 3° and 6° slopes reveals an increase in maximum bending moment by approximately 1.3-1.45 times for the downslope and upslope piles, respectively. For the KI-only condition, the corresponding increases are approximately 1.6 times for the upslope piles and 1.9 times for the downslope piles. These differences are primarily attributed to the enhanced kinematic demands imposed by greater lateral soil displacement at steeper slope inclinations.

4 CONCLUSIONS

Two dynamic centrifuge tests were conducted to investigate the effect of slope inclination on the seismic response of pile groups in layered soil comprising soft clay overlying dense sand. Despite the modest change in slope angle from 3° to 6°, barely perceptible to the naked eye, the resulting increase in soil deformation was substantial. The lateral ground displacement for a 6° slope was approximately three times greater than that for a 3° slope, demonstrating the strong sensitivity of seismic-induced soil movement to even minor variations in slope geometry.

The bending moment response of the pile groups reflected this heightened kinematic demand. In all cases, the maximum bending moment occurred slightly below the clay–sand interface due to the sharp contrast in the stiffness between the two layers. Upslope piles consistently exhibited the highest bending moments, while downslope piles experienced 22–34 % lower values as a result of group shadowing effects. The introduction of head mass led to a notable amplification of bending, with peak moments increasing by about twofold compared with the kinematic-only condition. Increasing the slope angle from 3° to 6° further intensified bending by up to 45%, primarily due to the larger lateral soil displacements mobilised at steeper inclinations.

Taken together, the results emphasise that modest differences in slope geometry can significantly alter both soil deformation patterns and pile bending demands. Designers should therefore treat gentle slopes with the same scrutiny as steeper ones, ensuring that kinematic interaction effects and layer stiffness contrasts are appropriately represented in analysis. Future work extending these observations across a wider range of slope angles and soil profiles would help refine design guidance for pile groups in complex topography.

REFERENCES

Brennan, A., Madabhushi, S.P.G. and Houghton, N.E. (2006). Comparing laminar and equivalent shear beam (ESB) containers for dynamic centrifuge modelling. *Physical Modelling in Geotechnics*. https://doi.org/10.1201/noe0415415866.ch17

Garala, T.K. and Madabhushi, S.P.G. (2021a). Influence of the phase difference between kinematic and inertial loads on seismic behaviour of pile foundations embedded in layered soils. *Canadian Geotechnical Journal*, 58(7): 1005–1022. https://doi.org/10.1139/cgj-2020-0346

Garala, T.K. and Madabhushi, S.P.G. (2021b). Role of pile spacing on the dynamic behaviour of pile groups in layered soils. *Journal of Geotechnical and Geoenvironmental Engineering*, 147(3). https://doi.org/10.1061/(ASCE)GT.1943-5606.0002462

Haigh, S.K. (2002). Effects of earthquake-induced liquefaction on pile foundations in sloping ground. PhD thesis, University of Cambridge.

Hardin, B. O., & Drnevich, V. P. (1972). Shear modulus and damping in soils: *Design equations and curves*. *Journal of the Soil Mechanics and Foundations Division*, *98*(7), 667–692. https://doi.org/10.1061/JSFEAQ.0001760

Haskell, J.J.M., Madabhushi, G.S.P., Cubrinovski, M. and Winkley, A. (2013). Lateral spreading-induced abutment rotation in the 2011 Christchurch earthquake: Observations and analysis. *Géotechnique*, 63: 1310–1327. https://doi.org/10.1680/geot.12.P.174

Lau, B.H. (2015). Cyclic behaviour of monopile foundations for offshore wind turbines in clay. PhD thesis, University of Cambridge.

Madabhushi, G.S.P. (2014). *Centrifuge Modelling for Civil Engineers*. CRC Press. https://doi.org/10.1201/9781315272863

Madabhushi, G.S.P., Houghton, N.E. and Haigh, S.K. (2006). A new automatic sand pourer for model preparation at the University of Cambridge. Proceedings of the 6th International Conference on Physical Modelling in Geotechnics (ICPMG'06), pp. 217–222.

Madabhushi, G.S.P., Houghton, N.E., Haigh, S.K. and Schofield, A.N. (2012). Development of a servo-hydraulic earthquake actuator for the Cambridge Turner beam centrifuge. *International Journal of Physical Modelling in Geotechnics*, 12(2): 77–88.

Nadim, F., G. Biscontin, and A. M. Kaynia. n.d. "Seismic Triggering of Submarine Slides." Paper presented at the Offshore 521 Technology Conference, Houston, TX, April 30–May 3, 2007.

Schofield, A.N. (1980). Cambridge Geotechnical Centrifuge Operations. *Géotechnique*, 30(3): 227–268.

Soriano Camelo, C.Y., Almeida, M.C.F., Almeida, M.S.S., Madabhushi, G.S.P. and Stanier, S. (2022). Centrifuge modelling of the seismic behaviour of soft clay slopes. Journal of Geotechnical and Geoenvironmental Engineering, 148(11). https://doi.org/10.1061/(ASCE)GT.1943-5606.0002884

Viggiani, G. and Atkinson, J.H. (1995). Stiffness of fine-grained soil at very small strains. *Géotechnique*, 45(2): 249–265. https://doi.org/10.1680/geot.1995.45.2.249